

The relativistic Fe emission line in XTE J1650–500 with *BeppoSAX*: evidence for black hole spin and light bending effects?

G. Miniutti¹*, A.C. Fabian¹, J.M. Miller^{2,3}

¹ Institute of Astronomy, University of Cambridge, Madingley Road, Cambridge CB3 0HA

² Harvard-Smithsonian Center for Astrophysics, 60 Garden Street, Cambridge MA 02138, USA

³ NSF Astronomy and Astrophysics Postdoctoral fellow

22 May 2019

ABSTRACT

We report spectral results from three *BeppoSAX* observations of the black hole candidate XTE J1650–500 during its 2001/2002 outburst. We find strong evidence for the presence of a broad and strongly relativistic Fe emission line. The line profile indicates an accretion disc extending down to two gravitational radii (or less) suggesting the presence of a rapidly rotating central Kerr black hole. Thanks to the broadband spectral coverage of *BeppoSAX*, we could analyze the 1.5–200 keV spectra of the three observations and report the presence of a strong reflection component from the accretion disc, which is totally consistent with the observed broad Fe emission line. The shape of the reflection component appears to be affected by the same special and general relativistic effects that produce the broad Fe line. We study the variation of the different spectral components from the first to the third observation and we find that they are well reproduced by a recently proposed light bending model.

Key words: black hole physics — X-rays: individual (XTE J1650–500) — X-rays: stars

1 INTRODUCTION

Black Hole Candidates (BHC) often exhibit transitions between different X-ray states, defined by their different spectral and temporal behaviour (Tanaka & Lewin 1995; van der Klis 1995; Méndez & van der Klis 1997; McClintock & Remillard 2003). Transitions between different X-ray states are believed to be mainly due to variations in the mass accretion rate. However, recent observations (see e.g. Homan et al. 2001) strongly suggest that a single parameter is not sufficient to explain the nature of the different states, and at least a second one must be considered, whose nature is still unclear.

Black hole X-ray binaries appear to evolve through a continuous range of states whose general properties strongly depend on the relative contribution and interplay between two main spectral components, i.e. a soft thermal disc component and a hard non-thermal power law component. In some cases the presence of a reflection component and/or of emission lines and edges has been observed suggesting reprocessing of the hard X-rays by cold material (generally identified with the accretion disc). The so-called hard state is dominated by the non-thermal component and is separated from the soft state, in which the thermal component dominates, by an intermediate one where the power law and the thermal component contribute approximately by the same amount to the X-ray spectrum.

Here we report spectral results from three *BeppoSAX* observa-

tions of the BHC XTE J1650–500 during its 2001/2002 outburst. The X-ray transient XTE J1650–500 was first detected in outburst with the *Rossi X-Ray Timing Explorer* (RXTE) on 2001 September 5 (Remillard 2001). Optical and radio counterparts were identified by Castro-Tirado et al. (2001) and Groot et al. (2001), respectively. Subsequent observations revealed X-ray variability, a hard spectrum and quasi-periodic oscillations (QPOs) at a few Hz making the source a BHC, although the mass of the central object is still not well constrained by the data (Markwardt, Swank & Smith 2001; Revnivtsev & Sunyaev 2001; Wijnands, Miller & Lewin 2001).

High frequency variability at about 250 Hz (and also likely at $250 \times 2/3$ Hz) has been detected during the transition from the hard to the soft state (Homan et al. 2003) confirming that high frequency QPOs in black hole systems are predominantly observed when neither the thermal nor the power law component completely dominate the energy spectrum. If the 250 Hz oscillation is interpreted as the orbital frequency at the innermost stable circular orbit, one can obtain a mass estimate of $8.2 M_{\odot}$ for a non-rotating black hole. If a rotating black hole is considered, the black hole mass could well be much higher.

XMM-Newton observations close to the peak of the outburst in the very high state revealed the presence of a broad and asymmetric Fe emission line suggesting that the black hole in XTE J1650–500 is a rapidly rotating Kerr black hole (Miller et al. 2002a). Fe line diagnostics is potentially very important for constraining the accretion flow geometry, black hole spin and the presence of centrally concentrated primary sources of hard X-rays. Evidence of broad, relativistic Fe lines is found in several BHC (see for example Mar-

* E-mail: miniutti@ast.cam.ac.uk

tocchia et al. 2002; Miller et al. 2003, 2002a,b,c) and AGN (see e.g. Tanaka et al. 1995; Wilms et al. 2001; Fabian et al. 2002 for the most remarkable case of MCG-6-30-15).

The *BeppoSAX* observations of the 2001/2002 XTE J1650–500 outburst were performed just before and after the *XMM-Newton* observation that revealed the presence of a relativistic Fe emission line. Thus, our main purpose is to explore the Fe line energy band to confirm (or not) the *XMM-Newton* detection and to obtain improved constraints from the broadband spectra; thanks to the broadband coverage of the *BeppoSAX* instruments, we present a self-consistent analysis of the 1.5–200 keV spectrum XTE J1650–500 during its 2001/2002 outburst.

2 OBSERVATION

XTE J1650–500 was observed 3 times by the Italian–Dutch satellite *BeppoSAX* (Boella, Butler & Perola 1997a) during 2001. Here we report on the three observations made on September 11 (obs. 1), September 21 (obs. 2) and October 3 (obs. 3). For comparison, we note that the *XMM-Newton* observation by Miller et al. 2002 that revealed the presence of a broad, relativistic Fe line was performed on September 13. In this paper, data from the imaging instruments (LECS Parmar et al. 1997 and MECS Boella et al. 1997b) and from the collimated PDS (Frontera et al. 1997) instrument are reported. The data files have been obtained from the *BeppoSAX* public archive. Spectra for the LECS and MECS instruments are obtained within a circular region centred on the source with radius of 8 arcmin. The background was extracted from event files of source-free regions of the same size. Net exposures times for LECS were of 6.8 ks, 20.3 ks and 14.1 ks (obs. 1,2 and 3 respectively), while the MECS exposures were of 27.8 ks, 47.4 ks and 63.9 ks. The PDS exposure times were of 21.4 ks, 30.7 ks and 12.5 ks. The *BeppoSAX* data were fitted by using the XSPEC 11.2 package (Arnaud 1996). In the following, all the quoted uncertainties on the parameters correspond to 90 per cent confidence intervals for one interesting parameter ($\Delta\chi^2 = 2.71$).

3 SPECTRAL ANALYSIS

We first analysed the MECS data in the 2.5–10 keV energy band in order to look for the presence of a broad Fe emission line as observed in the September 13 *XMM-Newton* observation by Miller et al. 2002. Some feature is present in the MECS data below 2.5 keV, independently of the spectral model that is used to analyse the data. We thus decided to ignore the low energy data below 2.5 keV and focus on the iron line energy band. To better constrain the continuum and to assess the relevance of reflection components in the spectra, we then added the PDS data in the range 13–200 keV. Some data from the LECS instruments (1.5–3.0 keV) have also been considered and we report our analysis of the broadband 1.5–200 keV data (LECS + MECS + PDS).

3.1 The 2.5–10 keV spectrum from the MECS instrument

We first analysed the MECS data by considering the “standard” model for galactic black hole candidates X-ray sources, i.e. a multi-colour accretion disc blackbody (MCD) from Mitsuda et al. (1984) and a power law, modified by absorption in the interstellar medium (the PHABS model in XSPEC). The fit is very poor for the first two observations ($\chi^2 = 958$ and $\chi^2 = 422$, respectively) and better for

obs. 3 ($\chi^2 = 201$) for 156 degrees of freedom. The main reason for the low quality of the fits is the presence of large residuals in the region of the Fe complex, above 3.5–4 keV. The shape of the residuals strongly suggest the presence of a broad and asymmetric Fe emission line in all the three observations.

We then describe the 2.5–10 keV MECS data by adding the LAOR model to account for relativistic iron line emission from an accretion disc around a Kerr black hole. In this model, the emissivity profile on the accretion disc is described by a power law of the form $\epsilon(r) = r^{-\beta}$, where the emissivity index β is a free parameter of the model. After some testing, the inclination was fixed to 45 degrees (as in Miller et al. 2002) as the data indicate clear preference for intermediate inclinations. The outer disc radius was fixed to its maximum possible value of $400 r_g$, where $r_g = G M/c^2$ and M is the black hole mass. The inner disc radius, the emissivity index, the rest energy of the emission line, and the model normalisation were let free to vary during the fit. A smeared edge (the SMEDGE model, see Ebisawa et al. 1994) was also added to the model.

In Fig. 1, to demonstrate the presence of the broad Fe line in the data, we show the data/model ratio obtained by removing the LAOR component and ignoring the 3.5–7.5 keV band in fitting the model. The broad residuals shown in Fig. 1 imply that a relativistic Fe emission line is present in the data, confirming its detection with *XMM-Newton* by Miller et al. (2002).

The addition of the SMEDGE and LAOR components significantly improved the fit ($\chi^2 = 159.0$, $\chi^2 = 197.5$, and $\chi^2 = 148.6$ for obs. 1, 2, and 3 respectively, for 150 degrees of freedom) with respect to our initial model (DISKBB + POWERLAW). The results of the spectral analysis are reported in Table 1 as MODEL 1.

Taking into account the three observations, the effective neutral hydrogen column density is found to be $N_H = (0.52 \pm 0.13) \times 10^{22}$ atoms cm $^{-2}$. The LAOR model indicates the presence of a relatively strong and highly relativistic iron line with equivalent width in the range $EW \simeq 190 - 300$ eV in the three observations. The line energy in obs. 2 and 3 is consistent with a high level ionisation, while in obs. 1 it suggests emission from less ionised, almost neutral, iron.

The emissivity profile on the accretion disc is well described by a steep power law with index $\beta \simeq 4.5$. This steep emissivity is consistent with measurements by *XMM-Newton* (Miller et al. 2002a) and strongly suggests that the accretion disc is illuminated by a centrally concentrated, relatively small source of primary hard X-rays. This primary source may be associated for example to rotational energy extraction from the central black hole (Blandford & Znajek 1977) and/or to the presence of an aborted/weak X-ray jet.

The Fe emission line is consistent with emission from an accretion disc extending down to about $2 r_g$. Such a small inner disc radius is not compatible with a non-rotating Schwarzschild black hole if the accretion disc is assumed to extend down to the marginal stable orbit ($6 r_g$ for a Schwarzschild black hole). On the other hand, since the marginal stable orbit for a maximally rotating Kerr black hole has a radius of about $1.24 r_g$, the data suggest the presence of a central rapidly rotating Kerr black hole.

If the inner disc radius is fixed to $6 r_g$, the χ^2 significantly worsen in all the three observations. Taking into account the three observations, we obtain a minimum χ^2 difference of about 17 (for one more degree of freedom), which means that an inner radius of $6 r_g$ can be rejected at least at the 4σ level of confidence. However, in obs. 1, we note that the best fit inner radius ($2 r_g$) is preferred over $6 r_g$ at a level of more σ than we can actually compute. A possible explanation, alternative to the one that invokes the presence of

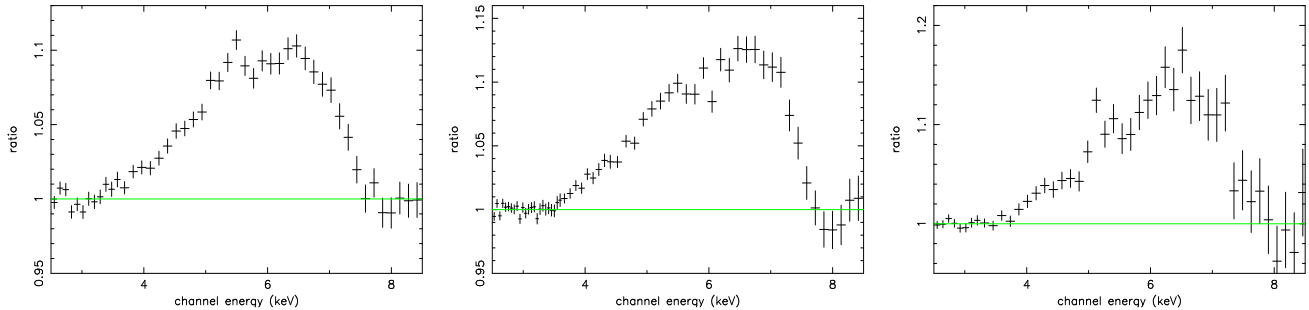


Figure 1. Detail in the Fe line region of the MECS data/model ratio obtained with a multicolour disc black body component, a power law and a smeared edge modified by photoelectric absorption for the three *BeppoSAX* observations (observations 1, 2, and 3, from left to right). The 3.5–7.5 keV band, where emission line features are expected, has been ignored in fitting the model. Ratios have been rebinned for visual clarity.

a Kerr black hole, is provided by the work of Reynolds & Begelman (1997). The authors showed that a the line profile from an accretion disc around a Schwarzschild black hole can be very similar to the one computed in the Kerr spacetime, if emission within the marginal stable orbit (the so called plunging region) is considered (but see Young, Ross & Fabian 1998).

3.2 The broadband 1.5–200 keV spectrum of XTE J1650–500

In order to constrain as well as possible the Fe line parameters, a careful analysis of the underlaying continuum is necessary. It is clear that a power law and a SMEDGE model are too simple, and probably rough, approximations to the hard spectral shape. In particular, the presence of the Fe line strongly suggests that a reflection continuum due to reprocessing of the primary X-rays by the accretion disc, is present in the data. This reflection component should be able to account for the absorption edge in a self-consistent manner, i.e. without any need for the phenomenological SMEDGE model.

However, the 2.5–10 keV energy band is too limited to constrain the reflection continuum. For this reason, we consider now the high energy data from the PDS instrument as well (in the range 13–200 keV) with the aim of revealing the presence of a reflection component in the spectrum. We also add some low energy data (1.5 to 3 keV) from the LECS instrument, to better constrain the thermal component of the spectrum. At lower energies, some absorption/emission features are visible. We decide to ignore these features in this analysis that is focused on the Fe complex and does not benefit much from the data below 1.5 keV. In this Section, we report our results on the 1.5–200 keV spectrum of XTE J1650–500.

The extension of the previous model (MODEL 1) to the 1.5–200 keV band does not provide a very good description to the data. The main reason is the presence of spectral curvature and positive residuals above 15–20 keV. The shape of the residuals suggests the presence of a Compton hump at about 20–30 keV due to a reflection component. Because of the presence of these residuals and of the relativistic Fe emission line, and anticipating the presence of a ionised disc as suggested by the Fe line rest energies (see Table 1), we add a reflection component (PEXRIV, from Magdziarz & Zdziarski 1995) to our model, and remove the phenomenological SMEDGE model.

Moreover, as all the components emitted from the accretion disc should be affected by the same relativistic effects, the reflection component, the thermal disc black body component and a narrow (i.e. with fixed zero width) Gaussian emission line are rela-

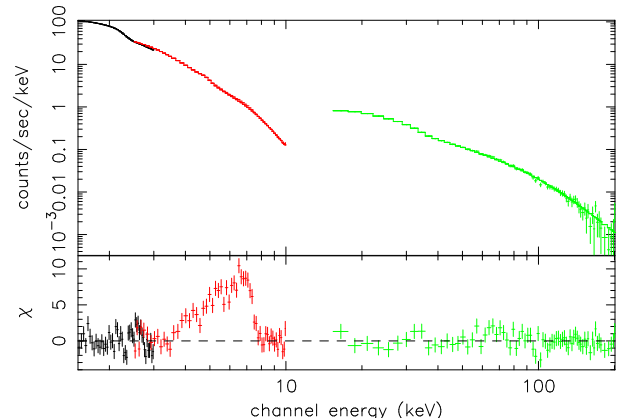


Figure 2. The 1.5–200 keV spectrum of obs. 2 and the data/model ratio (in terms of σ) obtained with our MODEL 2 when the normalization of the LAOR model is set to zero. The presence of the relativistic Fe line is manifest. The data have been rebinned for visual clarity.

tivistically “blurred” by convolving it with the core of the LAOR model. The width of the Gaussian emission line is fixed to zero because the Fe line profile is dictated by the effects of the relativistic blurring; our description of the Fe emission line is completely equivalent to the one provided by the LAOR model. The incident continuum is described by a power law with high energy cutoff; the photon index, cutoff energy and normalization are tied to those of the PEXRIV model.

Summarizing, we are describing the data with a power law (with high energy cutoff) that illuminates both the accretion disc and the observer at infinity, and by thermal and reflection components (reflection continuum and Fe line) from the accretion disc itself. All the components emitted from the disc are affected by the same relativistic effects arising in a disc around a rotating Kerr black hole. We believe that this setup increases the self-consistency of this model (hereafter MODEL 2).

All abundances in the reflection model were fixed to solar values while the relative normalisation between incident power law and reflection (the relative reflection R) was let free to vary during the fit. The outer disc radius was fixed at $400 r_g$ and the inclination at 45 degrees, as before. We notice also that the same model was used by Miller et al. 2002 to describe the September 13 *XMM-Newton* data.

This model works well on the data of obs. 2 and 3 ($\chi^2/dof = 527.5/436$ and $\chi^2/dof = 440.7/418$, respectively) but a good fit can be obtained for obs. 1 only up to about 60 keV ($\chi^2/dof = 336.0/326$). If higher energy data are included, MODEL 2 fails to give an appropriate description of obs. 1. We shall report now our results with MODEL 2, restricting the energy band to 1.5–60 keV for obs. 1, and discuss later in more detail the broadband spectrum for this first observation. The results of the fits with MODEL 2 are reported in Table 2.

The photon index of the power law component is now consistent with the expected value and with previous observations of the XTE J1650–500 2001/2002 outburst and is much better constrained by the analysis. The data support the presence of a large reflection component with relative reflection in the range $R \simeq 1–3$, although these values are not very well constrained. Such large values of the relative reflection mean that the accretion disc is viewing more illuminating radiation than we actually detect in the power law component. We will discuss how this may be explained in the next Section. The surface disc temperature and the ionisation parameter (ξ) of the reflection model vary in the range $1–9 \times 10^6$ K and $0.2–1.6 \times 10^4$ erg cm/s, respectively. Although these values are not well constrained by the data a trend of increasing ξ from obs. 1 to 3, is observed (see Table 1).

Once again, the most relevant results concern the broad iron emission line. In all observations, the line emission is consistent with the disc extending down to 2 gravitational radii suggesting the presence of a rapidly rotating Kerr black hole. An inner radius of $r_{in} = 1.24 r_g$ (innermost stable orbit for a maximally rotating Kerr black hole) is preferred over $r_{in} = 6 r_g$ (innermost stable orbit for non-rotating Schwarzschild black hole) at the 4σ level or more in all observations. We stress again that r_{in} is measured not only through the iron line but is the result of the fit on all the components that are thought to originate from the accretion disc (thermal and reflection components) that are blurred with relativistic effects, so that the significance of the measured r_{in} is, in our opinion, enhanced.

The line EW varies in the range 150–220 eV, depending on the observation. The EW is smaller than in the previous analysis of the 2.5–10 keV data. This is mainly due to the non negligible contribution of the (ionised) reflection continuum in the Fe line region. The emissivity profile of the disc is quite steep ($\beta \approx 3.7$) suggesting that the iron line emission is concentrated in the inner regions of the accretion disc.

Summarising, our results confirm the evidence for the presence of a Kerr black hole rotating close to its maximum possible angular momentum ($a = 0.998$) in XTE J1650–500 as shown in the *XMM-Newton* observation by Miller et al. (2002), although other interpretations may still be viable (Reynolds & Begelman 1997). As an example, the broadband 1.5–200 keV spectrum of obs. 2 is shown in Fig. 2: the normalization of the Fe emission line has been set to zero, in order to show the significance of the broad, relativistic line of XTE J1650–500.

We notice also a gradual increase of the relative reflection R from obs. 1 to 3 (see Table 1). We shall discuss this behaviour in terms of the correlation properties between the illuminating continuum (the power law) and the reflection components (the reflection continuum and the iron line) in the last Section. Here we only point out the the line equivalent width (computed with respect to the underlying total continuum) does not seems to correlate with the relative reflection (see Table 2). The uncorrelated variation of the line EW and R challenges the standard picture of reflection models because iron line and reflection continuum emission are thought to be

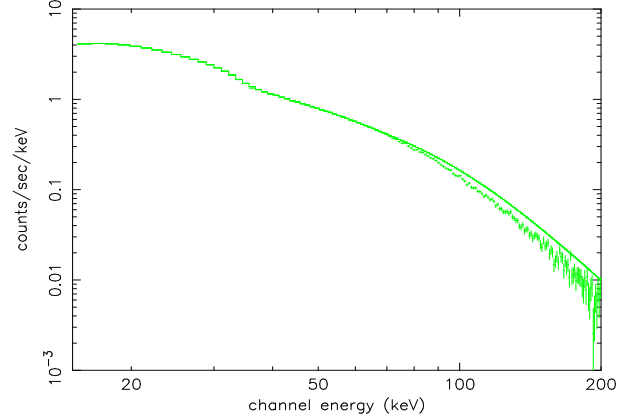


Figure 3. The 15–200 keV spectrum of obs. 1 from the PDS instrument demonstrates that our MODEL 2 is inappropriate to describe the data above 60–70 keV. A much sharper cutoff than the one provided by the CUTOFFPL model is needed.

different aspects of the same physical phenomenon (i.e. reprocessing of the primary X-rays irradiating the accretion disc) and should be correlated.

3.3 The 1.5–200 keV spectrum of observation 1

As we already mentioned, MODEL 2 does not provide a good description of obs. 1 if data above 60 keV are included in the analysis. However, we think that the potential of broadband spectra in constraining the hard continuum (and, in particular the reflection components) is of vital importance with respect to self-consistent Fe line diagnostics, which is the main purpose of this work. In this Section, we explore the reason of the failure of MODEL 2 and suggest a possible solution.

The reason of the failure is clearly shown in Fig. 3, where we show the PDS spectrum when the 1.5–60 keV best fit model for obs. 1 (see Table 2) is extended up to 200 keV. The data in obs. 1 clearly require a sharper cutoff above 60 keV than the one provided by the exponentially decaying power law and reflection. Even if the high energy cutoff of the CUTOFFPL and PEXRIV models is forced to assume low values, a reasonable fit can not be found.

It is possible that the sharper cutoff can be described by a steepening of the power law photon index above about 60 keV. To test this possibility, we replace the PEXRIV + CUTOFFPL model with the BEXRIV + BROKENPL one; the latter model (MODEL 3) assumes that the incident continuum is a broken power law and computes the reflection spectrum accordingly. The results of MODEL 3 are reported in Table 3.

The model provides a very good description to the broadband spectrum of the first *BeppoSAX* observation (with $\chi^2/dof = 441.2/450$). The results on the 1.5–200 keV broadband spectrum confirm the 1.5–60 keV analysis of the previous section without significant changes of the parameters. The difference is the presence of a break energy at about 70 keV where the photon index changes. Above that energy, the photon index steepens from $\Gamma_{low} \approx 1.8$ to $\Gamma_{high} \approx 2.6$. As no broken power law is needed to describe obs. 2 and 3, the break energy possibly moved towards high energies during the evolution of the XTE J1650–500 outburst. A different possibility is that the $\Delta\Gamma$ between the two photon index decreased with time during the outburst so that the index difference

is not detectable anymore in obs. 2 (performed ten days after obs. 1) and 3 (24 days after obs. 1).

4 CORRELATIONS BETWEEN ILLUMINATING CONTINUUM AND REFLECTION COMPONENTS

In this Section, we investigate the correlations (if any) between the Power Law Component (PLC) that illuminates the accretion disc and the reprocessed Reflection Dominated Component (RDC), i.e. reflection continuum and the iron line.

In the three observations, we observe that the contribution of the black body component to the total flux gradually increases with time, while the PLC contribution shows the opposite trend. The 1.5–200 keV flux of the black body component increases from 1.5×10^{-9} to 11.9×10^{-9} ergs/cm²/s, while the PLC flux decreases from 1.1×10^{-8} to 1.1×10^{-9} ergs/cm²/s. The relative reflection R increases by about a factor 3 as the PLC decreases from obs. 1 to 3 suggesting the R is anti-correlated with the PLC flux. Moreover, the iron line EW shows an erratic behaviour and does not correlate with R or with the PLC, challenging the usual picture of reflection from irradiated discs.

Our results are difficult to explain in the framework of the standard view of reflection models because any RDC emitted from the accretion disc is expected to respond to changes in the illuminating flux (the PLC). Furthermore, the line EW should be correlated with the relative reflection since both the Fe line and the reflection continuum are thought to originate from reprocessing of the illuminating continuum in the accretion disc.

However, this picture is probably oversimplified and fails (for example) to account for the variability of the Seyfert 1 galaxy MCG–6–30–15. As already pointed out by Miller et al. (2002), this AGN exhibits some clear similarities with XTE J1650–500. In particular, it is characterised by an extremely broad iron emission line (strongly suggesting the presence of a Kerr black hole) and a steep emissivity profile (Wilms et al. 2001; Fabian et al. 2002). MCG–6–30–15 exhibits also a peculiar variability behaviour: in its normal states the spectral variability can be accounted for by a phenomenological model comprising a PLC that varies in normalisation and an almost constant RDC (and iron line) (Shih, Iwasawa & Fabian 2002; Fabian & Vaughan 2003; Taylor, Uttley & McHardy 2003). In low flux states, the iron line seems to be slightly broader, and correlated with the PLC (Reynolds et al. 2003). This behaviour has been successfully reproduced in terms of a light bending model in which general relativistic effects strongly affect the emission in the near vicinity of the central Kerr black hole (Miniutti et al. 2003a; Miniutti & Fabian 2003b).

The basic idea of the light bending model is that the PLC variability is mostly due to changes in the height of a centrally concentrated primary source of hard X-rays above the accretion disc rather than to changes in its intrinsic luminosity. If the source height is small (few gravitational radii), most of the radiation is bent onto the accretion disc by the strong gravitational field of the central black hole: this strongly reduces the observed PLC at infinity and enhances the illumination of the disc. The Fe line (and any RDC) varies with much smaller amplitude than the PLC and different regimes can be identified in which the line is correlated with the PLC, almost constant, or anti-correlated with the PLC. These regimes correspond to low, medium and high PLC flux states.

The behaviour of the iron line flux with respect to the PLC flux in XTE J1650–500 has been measured with *RXTE* during the same

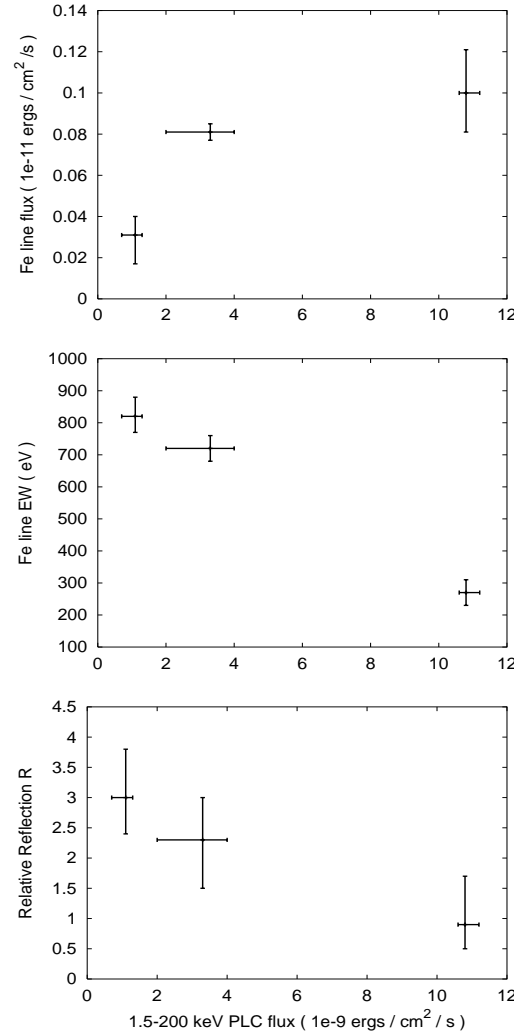


Figure 4. From top to bottom, we show the Fe line flux, the Fe line EW (with respect to the PLC only) and the relative reflection R as a function of the PLC flux in the 1.5–200 keV energy band. Errors correspond to 90 per cent confidence intervals.

2001/2002 outburst and results are reported by Rossi et al. (2003). The observed behaviour is remarkably similar to the predictions of the light bending model presenting a correlation of the Fe line with the PLC in low PLC flux states and an almost constant Fe line at higher PLC flux (see e.g. Figure 5 of Rossi et al. 2003 and Figure 2 of Miniutti & Fabian 2003b). Of course, this does not mean that light bending is really at work in this source and that other models can not explain the correlation properties. However, the strong similarity between theoretical predictions and observational data is manifest. More detail on the light bending model can be found in Miniutti et al. (2003a; 2003b).

A major prediction of the model is that the hard spectrum becomes more and more reflection dominated as the PLC drops (i.e. as the height of the primary source decreases) so that the relative reflection R increases as the system goes into low PLC flux states. Large values of the relative reflection are naturally expected in low PLC flux states.

If the PLC variability can be accounted for by light bending, the increase of the relative reflection (and its large value) as the PLC flux drops from obs. 1 to 3 can be understood. Moreover, as the

source height decreases and the PLC drops, the inner regions of disc are more and more illuminated, so that a reasonable expectation is that the ionisation parameter of the disc should increase. This may explain the trend of increasing ionization parameter from obs. 1 to 3 (see Table 2).

In the framework of the light bending model, the iron line EW should be correlated with R (and anti-correlated with the PLC flux with the exception of very low PLC flux states where a constant EW can be produced). We point out here that the latter prediction refers to the line EW with respect to the observed fraction of the continuum that illuminated the disc. This is represented by the observed PLC flux only. If the (ionised) reflection continuum or the thermal disc component contribute significantly to the Fe line energy band, the measured EW with respect to the total underlying continuum can be very different to that with respect to the PLC only.

As a test of the model, we then measure the Fe line EW with respect to the PLC only. The 1.5–200 keV flux of the black body, the PLC, the reflection continuum, and the Fe line are given in Table 2 together with the relative reflection R , and the Fe line EW with respect to the PLC only (EW_{PLC}). Our results suggest that the Fe line EW is anti-correlated with the PLC flux and positively correlated with the relative reflection R , in agreement with the predictions of the light bending model. In Fig. 4, we show the Fe line flux, the Fe line EW_{PLC} and the relative reflection R as a function of the 1.5–200 keV PLC flux. Clearly, three observations are not enough to establish correlations properties with high level of significance. However, we find it interesting that standard reflection models, once general relativistic effects are taken into account, can be sufficient to explain these otherwise puzzling observations.

5 DISCUSSION AND CONCLUSIONS

We present a self-consistent broadband spectral analysis of the BHC XTE J1650–500 during its 2001/2001 outburst. The three *BeppoSAX* observations cover about 25 days starting from 2001 September 11, only a few days after the peak of the outburst. From the results of our spectral analysis, we conclude that XTE J1650–500 was observed in the very high/intermediate state.

We have observed a broad Fe line profile in all three observations, confirming the detection with *XMM-Newton* by Miller et al. (2002a) during the same very high state on 2002 September 13. The Fe line profile we observe strongly suggests that the accretion disc extends down to $r_{in} \approx 2$, well within the limit of marginal stability for a non-rotating Schwarzschild black hole, thus indicating that XTE J1650–500 harbors a rapidly rotating (possibly maximally rotating) Kerr black hole.

The Fe line emission is consistently associated with a strong reflection spectral component from the accretion disc. The reflection dominated spectrum is also distorted by the special and general relativistic effects in the vicinity of the central black hole in the same way as the Fe line, by convolving it with the kernel of the LAOR model. Thanks to the broadband (1.5–200 keV) coverage, the reflection component helps to constrain the parameters of the LAOR model (mainly inner disc radius and emissivity index) in a much better way than if only the Fe line was considered.

The emissivity profile of the disc seems to be inconsistent with the energy dissipation expected from standard disc models ($\beta \approx 3$) and tends to be steeper, suggesting that the primary source that illuminates the disc is centrally concentrated.

From the first to the third observation, the power law component of the spectrum dropped by about one order of magnitude.

In the same time, the relative reflection increased by a factor 3, suggesting that the spectrum becomes more and more reflection dominated as the power law flux decreases. We interpret this behaviour in terms of a light bending model for the variability of X-ray sources that has been presented elsewhere (see Miniutti et al 2003a,b). Both the Fe line flux and EW correlate with the power law flux and relative reflection as predicted by this model. Our results on the Fe line-power law flux behaviour are consistent with the long term observations of XTE J1650–500 with RXTE as reported by Rossi et al. (2003).

ACKNOWLEDGEMENTS

GM thanks Kazushi Iwasawa for constructive discussions and Alessandra de Rosa for her help with *BeppoSAX* data analysis. We also thank the *BeppoSAX* Scientific Data Center. GM thanks the PPARC for support. ACF thanks the Royal Society for support. JMM thanks the NSF for support through its AAPF program.

REFERENCES

Arnaud K.A., 1996, in ASP Conf. Ser. 101: Astronomical Data Analysis Software and Systems V, 5, 17

Blandford R.D., Znajek R.L., 1977, MNRAS, 179, 433

Boella G., Butler R.C., Perola G.C., 1997a, A&AS, 112, 299

Boella G. et al. 1997b, A&AS, 112, 327

Castro-Tirado A.J., Kilmartin P., Gilmore A., Petterson O., Bond I., Yock P., Sanchez-Fernandez C., 2001, IAU Circ., 7707, 3

Fabian A.C. et al., 2002, MNRAS, 335, L1

Fabian A.C., Vaughan S., 2003, MNRAS, 340, L28

Fiore F., Guainazzi G., Grandi P., 1999, Cookbook for *BeppoSAX* NFI Spectral Analysis. SDC report (<http://asdc.asi.it/bepposax/software/index.html>)

Frontera F., Costa E., dal Fiume F., Feroci M., Nicastro L., Orlandini M., Palazzi E., Zavattini G., 1997, A&AS, 112, 357

Groot P., Tingay S., Udalski A., Miller J., 2001, IAU Circ., 7708, 4

Homan J., Wijnands R., van der Klis M., Belloni T., van Paradijs J., Klein-Wolt M., Fender R., Méndez M., 2001, ApJS, 132, 377

Homan J., Klein-Wolt M., Rossi S., Miller J.M., Wijnands R., Belloni T., van der Klis M., Lewin W.H.G., 2003, ApJ, 586, 1262

Markwardt C., Swank J., Smith E., 2001, IAU Circ., 7707, 2

Martocchia A., Matt G., Karas V., 2002, A&A 383, L23

McClintock J.E., Remillard R.A., to appear in Compact Stellar X-ray sources eds. W.H.G. Lewin and M. van der Klis, preprint (astro-ph/0306213)

Méndez M., van der Klis M., 1997, ApJ, 479, 926

Miller J.M. et al., 2002a, ApJ, 570, L69

Miller J.M., Fabian A.C., in't Zand J.J.M., Reynolds C.S., Wijnands R., Nowak M.A., Lewin W.H.G., 2002b, ApJ, 577, L15

Miller J.M. et al., 2002c, ApJ, 578, 348

Miniutti G., Fabian A.C., Goyer R., Lasenby A.N., 2003a, MNRAS, 344, L22

Miniutti G., Fabian A.C., 2003b, submitted to MNRAS, preprint (astro-ph/0309064)

Parmar A.N. et al. 1997, A&AS, 122, 309

Remillard R., 2001, IAU Circ., 7707, 1

Revnivtsev M., Sunyaev R., 2001, IAU Circ., 7715, 1

Reynolds C.S., Begelman M.C., 1997, ApJ, 488, 109

Reynolds C.S. et al. 2003, submitted to MNRAS

Rossi S., Homan J., Miller J.M., Belloni T., 2003, to appear in Proc. of the II *BeppoSAX* Meeting, May 5–8, van den Heuvel E.P.J., in't Zand J.J.M. and Wijers R.A.M.J. eds, Amsterdam, preprint (astro-ph/0309129)

Shih D.C., Iwasawa K., Fabian A.C., 2002, MNRAS, 333, 687

Tanaka Y. et al., 1995, Nature, 375, 659

Tanaka Y., Lewin W., 1995, in “X-ray Binaries”, Lewin W., van Paradijs J.,
van den Heuvel E. eds., Cambridge University Press, p. 126

Taylor R.D., Uttley P., McHardy I.M., 2003, MNRAS, 342, L31

van der Klis M., 1995, in “X-ray Binaries”, Lewin W., van Paradijs J., van
den Heuvel E. eds., Cambridge University Press, p. 252

Wijnands R., Miller J.M., Lewin W.H., 2001, IAU Circ., 7715, 2

Wilms J., Reynolds C.S., Begelman M.C., Reeves J., Molendi S., Staubert
R., Kendziorra E., 2001, MNRAS, 328, L27

Young A.J., Ross R.R., Fabian A.C., 1998, MNRAS, 300, L11

MODEL 1									
	Γ	KT_{rmin}	E_{Fe}	EW	β	r_{in}	E_{edge}	τ_{max}	χ^2/dof
2.5–10 keV SPECTRUM (MECS)									
obs. 1	$1.76^{+0.02}_{-0.03}$	$0.64^{+0.04}_{-0.03}$	$6.64^{+0.18}_{-0.14}$	260^{+30}_{-40}	$4.68^{+0.36}_{-0.27}$	$2.01^{+0.13}_{-0.62}$	$8.25^{+0.23}_{-0.22}$	$0.5^{+0.2}_{-0.1}$	159.0/150
obs. 2	$2.63^{+0.34}_{-0.22}$	$0.63^{+0.02}_{-0.03}$	$6.86^{+0.11}_{-0.21}$	300^{+30}_{-40}	$4.35^{+0.63}_{-0.54}$	$1.70^{+0.24}_{-0.46}$	$8.46^{+0.32}_{-0.59}$	$0.5^{+0.2}_{-0.2}$	197.5/150
obs. 3	$2.81^{+0.42}_{-0.34}$	$0.59^{+0.03}_{-0.04}$	$6.81^{+0.15}_{-0.37}$	190^{+40}_{-40}	$4.84^{+0.56}_{-1.24}$	$1.91^{+1.21}_{-0.67}$	$8.52^{+0.48}_{-0.74}$	$0.5^{+0.2}_{-0.2}$	148.6/150

Table 1. The 2.5–10 keV spectral analysis with MODEL 1

MODEL 2									
	Γ	KT_{in}	E_{Fe}	EW^4	β	r_{in}	R	ξ ($\times 10^4$)	χ^2/dof
1.5–200 keV SPECTRUM (LECS + MECS + PDS)									
obs. 1 (1.5–60 keV)	$1.81^{+0.09}_{-0.10}$	$0.64^{+0.07}_{-0.04}$	$6.45^{+0.11}_{-0.05}$	150^{+40}_{-30}	$3.52^{+0.14}_{-0.13}$	$1.31^{+0.56}_{-0.08}$	$0.81^{+0.8}_{-0.6}$	$0.2^{+0.2}_{-0.1}$	336.0/326
obs. 2	$2.14^{+0.03}_{-0.01}$	$0.67^{+0.02}_{-0.02}$	$6.72^{+0.12}_{-0.08}$	220^{+40}_{-40}	$3.88^{+0.12}_{-0.15}$	$1.68^{+0.16}_{-0.11}$	$2.3^{+0.7}_{-0.8}$	$1.0^{+0.9}_{-0.2}$	525.1/436
obs. 3	$2.08^{+0.06}_{-0.04}$	$0.63^{+0.04}_{-0.03}$	$6.61^{+0.17}_{-0.18}$	180^{+50}_{-40}	$3.79^{+0.29}_{-0.23}$	$2.08^{+0.29}_{-0.31}$	$3.0^{+0.8}_{-0.6}$	$1.6^{+1.3}_{-0.9}$	440.7/418
MODEL 3									
	Γ_{low}^5	KT_{in}	E_{Fe}	EW^4	β	r_{in}	R	ξ ($\times 10^4$)	χ^2/dof
1.5–200 keV SPECTRUM (LECS + MECS + PDS)									
obs. 1	$1.81^{+0.08}_{-0.10}$	$0.65^{+0.06}_{-0.05}$	$6.45^{+0.13}_{-0.05}$	160^{+40}_{-30}	$3.52^{+0.21}_{-0.15}$	$1.29^{+0.44}_{-0.05}$	$0.9^{+0.8}_{-0.4}$	$0.2^{+0.3}_{-0.1}$	441.2/450

¹ The parameters of the CUTOFFPL (BROKENPL) are tied to those of the reflection model PEXRIV (BEXRIV)² The relativistic blurring RELBLUR is provided by the kernel of the LAOR model³ The width of the NARROWGAUSS emission line is fixed to zero (see text for details)⁴ The Fe line EW is computed with respect to the total underlaying continuum (including the power law)⁵ Γ_{low} is the low energy photon index of the broken power law. The other relevant parameters are $E_{break} = 70.3^{+3.1}_{-2.4}$ and $\Gamma_{high} = 2.58^{+0.16}_{-0.12}$ **Table 2.** Top: The 1.5–200 keV spectral analysis with MODEL 2. The analysis has been restricted to the 1.5–60 keV energy band for obs. 1 (see text for details). Bottom: the 1.5–200 keV spectral analysis of obs. 1 with MODEL 3

1.5–200 keV FLUXES ¹ FROM THE BROADBAND BEST FIT MODELS							
	F_{tot}	F_{DiskBB}	F_{PLC}	F_{REFL}	F_{line}	R	EW_{PLC}
obs. 1	$25.9^{+0.9}_{-0.6}$	$1.5^{+0.3}_{-0.7}$	$10.8^{+0.4}_{-0.2}$	$6.0^{+1.7}_{-0.6}$	$10.0^{+2.1}_{-1.9}$	$0.9^{+0.8}_{-0.4}$	270^{+40}_{-40}
obs. 2	$18.9^{+0.8}_{-1.3}$	$11.4^{+0.4}_{-0.6}$	$3.3^{+0.7}_{-1.3}$	$4.1^{+1.0}_{-1.8}$	$8.1^{+0.4}_{-0.4}$	$2.3^{+0.7}_{-0.8}$	720^{+40}_{-40}
obs. 3	$14.9^{+0.6}_{-0.6}$	$11.8^{+0.8}_{-0.4}$	$1.1^{+0.2}_{-0.4}$	$1.9^{+0.6}_{-0.8}$	$3.1^{+0.9}_{-1.4}$	$3.0^{+0.8}_{-0.6}$	820^{+60}_{-50}

¹ Fluxes are in units of 10^{-9} erg/cm²/s with the exception of the Fe line flux which is in units of 10^{-11} erg/cm²/s**Table 3.** 1.5–200 keV unabsorbed flux of the main spectral components are shown together with the relative reflection and the Fe line EW computed with respect to the PLC only